

Stephen R. Macpherson\*, Godelieve Deblonde, Josep M. Aparicio, and Barbara Casati  
 Environment Canada, Atmospheric Science and Technology Directorate, Dorval, Canada

## 1. INTRODUCTION

Moisture fields in the troposphere have a high temporal and spatial variability. Over land, in situ observations consist of a network of surface and radiosonde observations (sparse) whereas space-based satellite observations of humidity are limited to the middle and upper troposphere. Observations from ground-based GPS meteorological networks (not affected by clouds or precipitation) provide a new high temporal (half hourly) source of atmospheric humidity information. The atmosphere has a significant impact on GPS satellite transmissions as it introduces a delay in the signal. This delay, when mapped to the zenith, is referred to as zenith troposphere delay (ZTD) and is estimated with relatively high accuracy in the processing of ground-based GPS network data for geodetic (precise positioning) applications.

ZTD is expressed as an excess path length rather than time delay (relative to signal transmission in a vacuum), and is on the order of 2 m. The main contribution to ZTD is the atmospheric mass, as measured by surface pressure  $P_s$  and is often called the zenith hydrostatic delay (ZHD). The remainder of the contribution, referred to as zenith wet delay (ZWD), depends strongly on the total amount of water vapour along the signal trajectory and weakly on the atmospheric temperature and can be as high as 0.4 m in very humid air masses. ZTD can be expressed as follows:

$$ZTD = f_1(\varphi, H) P_s + f_2(T_m) PW \quad (1)$$

where  $\varphi$  is the latitude,  $H$  is the height of the GPS antenna,  $PW$  is precipitable water, and  $T_m$  is vapour-weighted column mean temperature (which can be estimated from surface temperature  $T_s$ ). With observations of  $P_s$  and  $T_s$  from collocated (or nearby) weather stations,  $PW$  can be retrieved from ZTD observations (Bevis et al. 1992).  $PW$  varies from near zero to 70 mm.

The Global Systems Division (GSD) of the NOAA Earth System Research Laboratory (ESRL) maintains a research GPS meteorological network (Fig. 1) which was created in 1994 mainly from existing geodetic GPS networks in the US. Observations of  $P_s$ ,  $T_s$ , and surface relative humidity (RHs) are provided by collocated or nearby weather stations. GSD computes near-real-time (NRT) ZTD and with the  $P_s$  and  $T_s$  observations,

produces half-hourly  $PW$  observations. Sites are added yearly to the network (there are currently over 350 sites).

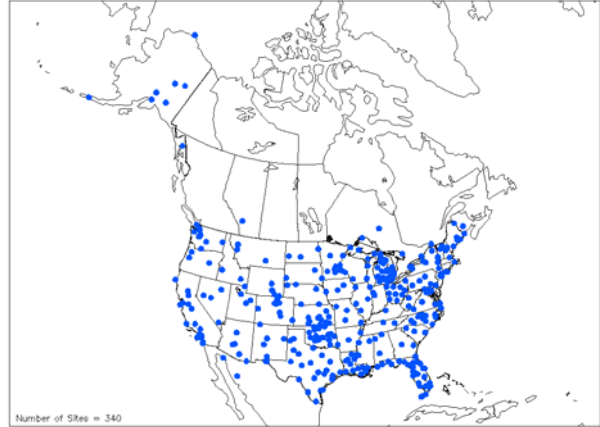


Figure 1: The NOAA/ESRL GPS meteorological network.

There is a similar GPS network in Europe, established as part of a European initiative called COST-716 to exploit ground-based GPS for climate and Numerical Weather Prediction (NWP) applications. Another source of GPS observations is the International GNSS Service (IGS), which produces ZTD for sites in their global network. Unlike the GSD network,  $P_s$  and  $T_s$  observations (and hence  $PW$ ) are not available at all the IGS and European sites. The data from these networks are freely available in NRT via the internet (ftp) or the Global Telecommunications System (GTS).

GPS  $PW$  accuracy is on the order of 1-2 mm (Deblonde et al. 2005), sufficient for assimilation in NWP. Either GPS  $PW$  or ZTD can be assimilated. To retrieve  $PW$  from ZTD, observations of surface pressure and temperature at the GPS sites are required (Eq. 1). It is preferable to assimilate ZTD directly as it is more straightforward to specify observation error and a bias correction.  $PW$  information can be extracted from ZTD by the assimilation system even if collocated surface observations of pressure and temperature are not available.

Environment Canada (EC) has been monitoring the GPS observations from the NOAA and European networks since 2004. Data impact experiments were carried out with NOAA/ESRL observations of ZTD,  $P_s$ ,  $T_s$ , and RHs and a research version of the EC Regional Analysis and Forecast System (RAFS). Results of these experiments are presented in this paper.

\* Corresponding author address: Stephen R. Macpherson, Environment Canada, Dorval, QC, Canada H9P 1J3; e-mail: [stephen.macpherson@ec.gc.ca](mailto:stephen.macpherson@ec.gc.ca)

## 2. GPS DATA ASSIMILATION

### 2.1 Background

In data assimilation for NWP, weather observations are optimally combined with a first-guess (short-range forecast) to produce an analysis which is used as the initial state for further forecasts. In variational assimilation, observations that are not analysis control variables are assimilated through an observation or forward operator. The forward operator maps the model state, defined by the analysis control variables (i.e. surface pressure, zonal and meridional winds, temperature, and humidity), into observation space. Assimilation of the observations leads to changes in the control variables.

Unlike radiosonde observations which are provided at specific pressure levels, measurements of GPS ZTD (and PW) provide no level-specific information. As a result, the first-guess error covariances and forward operator sensitivity to changes in the control variables determine the vertical distribution of the analysis increments (analysis minus first-guess). If the specified background errors are not representative of the actual background errors, the distribution of analysis increments may be sub-optimal.

The expected impact of assimilating ZTD is a significant reduction in specific humidity analysis error below 400 hPa and a much smaller impact on temperature and surface pressure analysis errors. An exception is when the first-guess state is very dry in which case ZTD is sensitive only to surface pressure (Eq. 1).

### 2.2 Data Impact Studies

The impact of real GPS observations on forecasts has been evaluated by NOAA/ESRL/GSD and by several centres in Europe. GSD studied (Gutman et al. 2004) the impact of assimilating the NOAA network GPS PW observations over the continental US (CONUS) on the National Centers for Environmental Prediction (NCEP) Rapid Update Cycle (RUC) analysis-forecast system (Benjamin et al. 2004). In these studies, an OI (optimum interpolation) type of approach is used for the assimilation and humidity analysis increments are restricted to the 500 hPa level and below.

The GSD studies show an overall positive impact on RH forecasts in the lower troposphere as well on precipitation accumulation forecasts. Improvements in 3h RH forecasts on the order of 6% (10% for US Midwest) below 500 hPa are observed. The improvement in RH forecasts is more evident in winter, when the humidity field is more uniform.

The improvement in precipitation forecast skill generally increases with the accumulation threshold amounts. Significant local improvements are also noted in specific cases, such as heavy precipitation events and severe storm development. Verification against GPS observations reveal lower RMSE and bias in forecast PW when GPS data are assimilated. The RMSE reduction is 25% at 3h and diminishes to 7.5%

after 12h, while the RUC model moist PW bias is reduced significantly.

Most of the studies in Europe were done as part of a project called TOUGH (Targeting Optimal Use of GPS Humidity measurements in meteorology). This project involves several research institutes, including the Danish Meteorological Institute (DMI), the Instituto Nacional de Meteorologia de Espana (INM), the Universita' degli Studi di L'Aquila (LAQ), the UK Met Office (MO), and Metéo-France. Observations are from the European (COST-716) GPS network consisting of close to 500 sites. The results are summarized in Vedel & Sattler (2006).

The institutes use a variety of assimilation methods (3D-Var, 4D-Var, nudging) and regional/mesoscale forecast models (HIRLAM model by DMI and INM, MM5 model by LAQ and the UK mesoscale model by MO). In all but one case (LAQ), ZTD is assimilated rather than PW. In the MO, INM and Metéo-France studies, site-dependent bias corrections are applied to the GPS observations prior to assimilation (based on mean differences from first-guess values).

Overall, the impact of ground-based GPS observations is found to be neutral to positive. Objective verification results vary somewhat between institutes, with positive impacts noted for lower tropospheric humidity, surface temperature, surface pressure, geopotential heights and precipitation accumulations. Some negative impacts were observed for small-threshold precipitation accumulations. All institutes report positive impacts for subjective (case-study) precipitation verification (both in distribution and amounts).

The 4D-Var tests at DMI highlight the importance of accounting for temporal observation error correlations when assimilating a time-series of observations. Positive impact on precipitation forecasts is only observed after the observation errors are increased to give proper weight to each observation in the time-series.

## 3. GPS OBSERVATIONS

The GPS observations assimilated in the experiments presented in this paper are taken from the NOAA/ESRL GPS meteorological network (Fig. 1) for summer and winter periods in 2004 and 2005. There were ~270 GPS sites in the network at the time. The observations that are assimilated are ZTD,  $P_s$ ,  $T_s$  and RHs, observed at 30-minute intervals. ZTD is produced for each site by GSD with the GAMIT (geodetic) software (King and Bock 2000) using a sliding-window data processing approach (Foster et al. 2005). RHs is converted to dewpoint depression (DPD) (temperature minus dewpoint temperature), which in turn is converted to the natural logarithm of specific humidity which is the control moisture variable of the EC analysis systems.

The EC analysis systems operate on a 6h cycle, so observations are grouped in 6h windows (centred at analysis times of 0000, 0600, 1200, 1800 UTC). For 30-minute GPS observations, this amounts to a time series of 12 observations per site at each analysis time. In our

data impact study, 3D-Var FGAT (First Guess at Appropriate Time) assimilation is employed to allow for assimilation of these time series of GPS observations. In 3D-Var FGAT, (O-F) values (or innovations) are obtained for a time-series of observations (O) and corresponding forecasts or first-guesses (F).

Estimates of observation error are required in data assimilation and determine the weight of the observation relative to the first-guess. These errors include both instrument and representativeness errors. ZTD observation error is made to vary with observed ZTD following a regression relation based on (O-F) monitoring statistics. For ZTD < 2.3 m (low PW and/or high elevation sites), the error is ~12 mm. The error increases for ZTD > 2.3 m, and is ~32 mm for ZTD of 2.6 m (high PW, low elevation sites).

Site-specific ZTD is obtained as part of an overall network solution (in a least-squares sense). The raw GPS data are based on signals received from a common set of GPS satellites. Assumptions in the GPS data processing have associated errors that affect solutions for all sites in the network. As a result, spatial and temporal ZTD observation error correlations exist, which must be accounted for in the assimilation process to avoid sub-optimal results.

The horizontal ZTD error correlations are found to be significant up to distances of 100-200 km (Eresmaa and Järvinen 2005). In the EC analysis systems, observations are thinned spatially to reduce the effects of horizontal (or vertical) observation error correlations (e.g. for wind profiler and satellite radiance observations). The same method is applied for GPS observations and thinning is performed that requires a minimum distance of 100 km between sites, which reduces the number of sites by ~30%.

Temporal ZTD error correlations are estimated and modelled by Stoew and Elgered (2005) for GPS sites in Sweden and Finland. They find a correlation e-folding time on the order of 1-2 days, attributed to systematic errors in the assumptions of the ZTD processing. At ECMWF, a method has been developed to account for temporal error correlations for 4D-Var assimilation (Järvinen et al. 1999). We use a similar method adapted to the special case of 3D-Var FGAT. The end-result is that a constant factor of 2.34 is applied to increase the ZTD observation error, which reduces the weight of each time-series observation in the 3D-Var analysis by an appropriate amount.

Another issue with GPS ZTD observations involves site-specific biases (in terms of mean O-F) as revealed in the monitoring. The biases can be quite significant in some cases (> 10 mm) with constant and variable components (variability on a scale of weeks to seasons, as well as diurnal). The existence of (O-F) type biases violates the basic assumptions of variational assimilation, with potentially negative impact on analyses. A dynamic, site-specific sliding window bias correction is applied to the ZTD at the pre-processing stage, as described in Section 6.  $P_s$  is bias corrected with the same approach. Other observations ( $T_s$  and RHs) are not bias corrected.

Observations are not assimilated if the difference between observation height and model surface topography exceeds specific limits, which are 800 m for  $P_s$  and  $T_s$ , 50 m for RHs, and 1000 m for ZTD. The low limit for RH means fewer surface RH observations are assimilated compared to the other variables. The analysis (model) values are adjusted to the observation height during assimilation for all observations except RH.

#### 4. ZTD OBSERVATION OPERATOR

The relevant analysis control variables are model surface pressure  $P_0$ , temperature  $T_i$ , and natural log of specific humidity ( $\ln q_i$ ),  $i = 1, 58$  vertical  $\eta$  levels, where  $\eta$  (a terrain following coordinate) is defined as:

$$\eta_i \equiv \frac{P_i - P_T}{P_0 - P_T},$$

where  $P_T$  is model top pressure (10 hPa). The observation operator is formulated in terms of  $q = e^{\ln q}$ .

The atmospheric refractivity for GPS satellite transmissions ( $N$ ) is given by

$$N = k_1 \frac{P_d}{T} + k_2 \frac{P_v}{T} + k_3 \frac{P_v}{T^2} \quad (2)$$

where  $P_d$  is dry air pressure,  $P_v$  is water vapour pressure,  $T$  is temperature and  $k_1$ ,  $k_2$  and  $k_3$  are refractivity constants (Bevis et al. 1994). ZTD is defined as:

$$ZTD \equiv \int_{z=sfc}^{toa} N dz \quad (3)$$

where sfc denotes surface, toa denotes top of atmosphere, and  $z$  is height above MSL.

ZTD is computed as the sum of the ZHD and the ZWD. Height  $z$  in Eq. 3 is converted to the analysis vertical coordinate  $\eta$  with application of the hydrostatic relation, and by using:

$$\begin{aligned} P_d &= P - P_v, \\ P_v &\approx \frac{qP}{\varepsilon}, \\ T_v &\equiv T \cdot (1 + \kappa q), \text{ and} \\ k_2' &= k_2 - \varepsilon k_1. \end{aligned}$$

ZHD and ZWD are respectively computed as follows:

$$ZHD = 10^{-6} \frac{R_d k_1}{g_m(\varphi, H)} P_0 \quad (4)$$

and

$$ZWD = 10^{-6} \frac{R_d}{g_0(\varphi) \varepsilon} (P_0 - P_T) \sum_{i=1}^{57} Nw_i (\eta_{i+1} - \eta_i) \quad (5)$$

where  $Nw_i$  is a mean layer wet refractivity term given by

$$Nw_i = (\bar{q}_i + \kappa \bar{q}_i^2) \left( k'_2 + \frac{k_3}{T_i} \right).$$

The over bars signify (i+1, i) layer averages,  $R_d$ ,  $\varepsilon$ ,  $\kappa$  are constants,  $g_m(\varphi, H)$  is mean column gravity as a function of latitude and surface height (above geoid), and  $g_0(\varphi)$  is surface gravity as a function of latitude.

The difference between the GPS antenna height and the model surface height ( $\Delta z$ ) is accounted for in the ZHD term (Eq. 4) through hydrostatic adjustment of the model surface pressure  $P_0$  to the GPS antenna height. The ZWD (Eq. 5) is adjusted to the antenna height by adding a correction term

$$\Delta ZWD = -\bar{N}_w \cdot \Delta z \quad (6)$$

where

$$\bar{N}_w = k'_2 \frac{\bar{P}\bar{q}}{\varepsilon\bar{T}} + k_3 \frac{\bar{P}\bar{q}}{\varepsilon\bar{T}^2}$$

is the mean wet refractivity. The over bars here refer to averages over the  $\Delta z$  layer, computed using  $P_0$  at antenna height from the ZHD adjustment, and assumed lapse rates for  $T$  and  $q$ . This method is similar to that proposed by Higgins (1999). For sites in the NOAA/ESRL network,  $|\Delta z|$  is < 100 m for ~85% of the sites, so the adjustments in most cases are relatively small.

## 5. THE REGIONAL ANALYSIS AND FORECAST SYSTEM

The data impact study uses the operational EC regional analysis and forecast system (called RAFS in this paper). The RAFS is separate from the main global data assimilation and forecast system, but shares the same observations (radiosonde, surface synoptic, aircraft, satellite winds and radiances, and US wind profiler). RAFS provides appropriate analyses for the EC regional (North America) GEM model (GEM-REG),

which provides two-day forecast guidance for Canadian public and aviation forecasts.

GEM-REG is the regional version of the Canadian Global Environmental Multiscale (GEM) model (Côté et al. 1998). The global version of GEM (GEM-GLB) is part of the EC 4D-Var global 6-hourly data assimilation system and provides long-range forecasts twice a day. It is a global uniform-grid model (0.45° longitude x 0.33° latitude) with 58 levels and physics described in Bélair et al. (2005). GEM-REG is a global variable-grid model with 58 levels. Resolution is high (~15 km) and uniform for a window centred over North America and drops off with distance outside the window. GEM-REG's schemes (Mailhot et al. 2005) for surface processes and deep convection are similar to those of GEM-GLB.

Twice a day, at 0000 and 1200 UTC (time  $t$ ), RAFS is launched with analyses from the global 4D-Var assimilation system that serve as initial conditions for a GEM-REG 6h forecast. The 6h forecast serves as the trial (first-guess) for 3D-Var FGAT data assimilation at time  $t+6h$  to create a new regional analysis. This analysis serves as initial conditions for a second GEM-REG 6h forecast, which becomes the trial for a second 3D-Var FGAT assimilation and regional analysis at  $t+12h$ . This is referred to as a 12h spin-up cycle. The two-day GEM-REG forecast is then run, with the final regional analysis as initial conditions. The whole cycle is repeated every 12h.

It is important to note that GPS observations are unique to RAFS in the data impact experiments. In other words, the global analyses that launch the RAFS are taken from global assimilation cycles that do not include GPS observations. This would not be the case in an operational setup, where so far the same observations are assimilated in both global and regional systems. Normally, when new observation types are added in data impact studies, the assimilation system is given a period of time (e.g. 2 weeks) to adjust to the new observation type. The products of the assimilation system for that period of time are not evaluated or verified. This could not be done in our RAFS experiments, so potential "new observation shocks" at the start of each RAFS cycle may have a negative impact.

## 6. EXPERIMENT SETUP AND GPS DATA PRE-PROCESSING

The two periods chosen for the study are July to September 2004 (summer) and December 2004 to February 2005 (winter). In the summer case, a series of 42 RAFS cycles were run, while in the winter case only 19 cycles were run. For both periods, the cycles were run twice, once with conventional observations only (the control) and once with GPS observations added (the experiment).

The results presented in this paper are for the summer runs only as the GPS observations have a more definite impact in summer months, when typical PW over North America is highest. For the limited number of cycles of the chosen winter period, observed impact on forecasts was much smaller and short-lived (<

12h). The summer control run is named RAM27 and the summer experiment run (with GPS) is RGP27.

Pre-processing of the GPS observations takes place before each assimilation in the RAFS cycles. In the following, (O-F) refers to the difference between the observations (O) and the FGAT F (3-9h forecasts). The pre-processing is done in five steps:

1. Update of the (O-F) database and re-computation of site-specific bias corrections
2. Application of the new bias corrections (to ZTD and  $P_s$ )
3. Background check of bias corrected observations (O-F)
4. Rejection of blacklisted observations
5. Spatial and temporal thinning of remaining observations (Section 3).

In step one, the current O-F values are added to a file containing all (O-F) values for each site and observation type, as well as the current site (O-F) statistics (mean and SD). Observations with very large (O-F) ( $> 6\sigma$ ) are assumed to be erroneous and are rejected. If enough observations are available over the last 10-20 day period, mean and SD (O-P) are re-computed. (The period is set to 10 days but can be extended back as far as 20 days if there are not enough observations.) These statistics are used to blacklist observations at sites where the mean or SD (O-P) is exceedingly high. Sites and associated observations are also blacklisted when there are too many rejections or when there are not enough observations to compute the statistics. The 10-20 day running-mean (O-F) for each site are applied as bias corrections in step 2. The blacklist information is applied in step 4.

The background check of step 3 is done for all observation types in the EC data assimilation systems. Observations are rejected if the (O-F) exceeds specified limits (based on the observation and background errors). The rejection for model-observation topography difference (section 3) is also done in this step.

The temporal thinning involves reducing the number of GPS time-series observations from 12 to 9 to match the FGAT times. In 3D-Var FGAT, the assimilation window of 6h is divided into 9 sub-windows centred at the valid times (FGAT times) of the 3-9h forecasts (available every 45 minutes) so that the 12 GPS observations per site in the 6h window are thinned to 9.

## 7. RESULTS

The results of the summer data impact experiments are presented in this section. In section 7.1, the direct impacts of GPS observations on the analyses of the RAFS are presented. Impacts on 00-48h forecasts of the GEM-REG model are presented in section 7.2.

### 7.1 Impacts on the regional analysis

Analysis impacts are evaluated for the second (final) analysis of the RAFS cycles only (valid at 0000 or

1200 UTC), which serves to initialize the 48h GEM-REG forecast.

Fig. 2 shows the standard deviation (SD) of the PW field differences between the control (RAM27) analysis and the experiment (RGP27) analysis over all 42 RAFS cycles. The SD is a measure of typical differences between the experiments. The main impact on analyses from the addition of GPS ZTD observations is expected to be on the integrated water vapour or PW. Impact is clearly evident in Fig. 2, where typical PW SD of 2-5 mm is observed. Maximum (absolute value) differences (not shown) are as high as 17 mm.

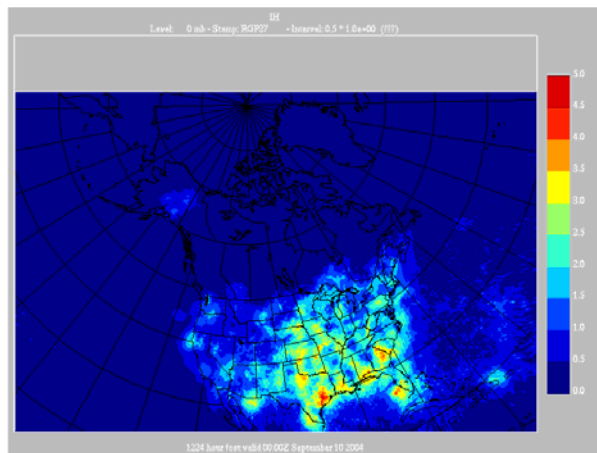


Figure 2: SD of Experiment minus Control analysis PW differences (units = mm). The scale ranges between 0 and 5 mm.

Impact on RH is evaluated by computing differences in the mean RH for three layers of the atmosphere: lower (surface to  $\eta$  level 0.7), middle ( $\eta$  level 0.7 to 0.4), and upper ( $\eta$  level 0.4 to 0.15). For a surface pressure of 1000 hPa, the layers roughly correspond to surface to 700 hPa, 700 hPa to 400 hPa and 400 hPa to 150 hPa respectively. Fig. 3 is the same as Fig. 2, but for lower layer mean RH. Here RH of SD differences of 5-10% are observed. Maximum differences (not shown) are as high as 50%. Similar differences are seen for middle and upper layers (not shown).

The mean of the PW and RH differences reveal biases between the experiment and the control. The mean PW differences are shown in Fig. 4. Biases on the order of 1-3 mm are evident in some regions. The PW biases are due mostly to biases in lower layer humidity (not shown) and may be due to residual biases in the ZTD observations (not removed by the bias correction scheme). Assimilation of surface DPD (without bias corrections) may also contribute to biases in lower troposphere humidity (surface biases will be spread upward through vertical background error correlations). The analyses (A) are verified against radiosonde observations (O) at a limited number of pressure levels. Fig. 5 shows the verification of analysis DPD for RGP27 (with GPS) and RAM27 (control). Levels where differences between the experiments are statistically significant ( $> 90\%$  confidence interval) are indicated by

green shading. Addition of GPS observations has a very small negative impact in DPD below 400 hPa. The larger impact at the 1000 hPa level can be attributed to assimilation of GPS surface DPD. There is also a small negative impact for 1000 hPa temperature (not shown). This type of negative impact on the analysis is also observed in a data impact study with observations of the US wind profiler network (St-James and Laroche 2005) and is to be expected when a new observation type is added which competes with the radiosonde data.

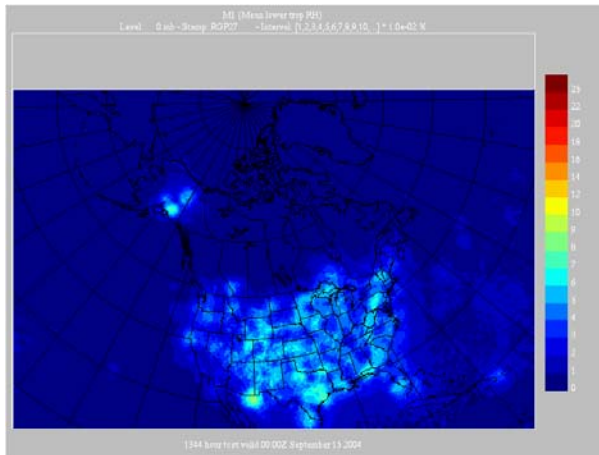


Figure 3: SD of Experiment minus Control analysis lower layer RH differences (units = %). The scale ranges between 0 and 25 %.

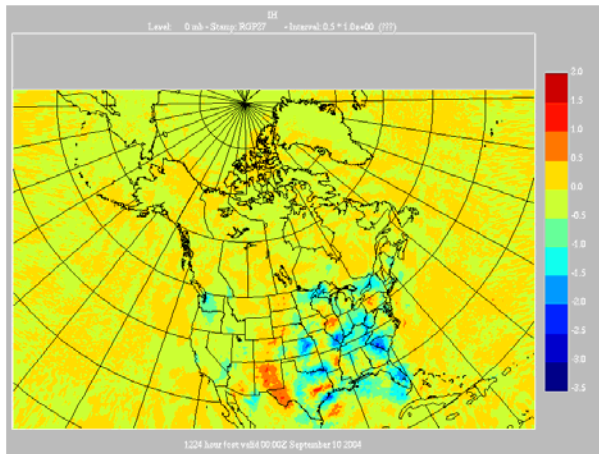


Figure 4: Mean of Experiment minus Control analysis PW differences (units = mm). The scale ranges between -3.5 and 2 mm.

Another impact of the GPS observations is seen in the geopotential height field (GZ). Fig. 6 shows the verifications of 6h forecast GZ against radiosonde observations (GZ plots are not available for the analysis). The entire GZ bias profile for experiment RGP27 (with GPS) is shifted to the right of the control by ~0.25 dam, which is due to a surface pressure bias difference of 0.35 hPa at analysis time between

experiment RGP27 (with GPS) and the control (see section 7.2).

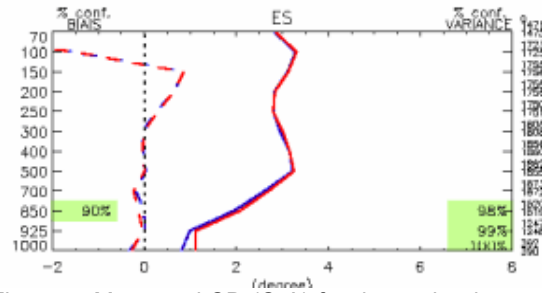


Figure 5: Mean and SD (O-A) for dew point depression, here labelled ES, for experiment (red lines) and control (blue lines), O denotes radiosonde observations. Dashed lines are mean (O-A) or bias and solid lines are SD (O-A).

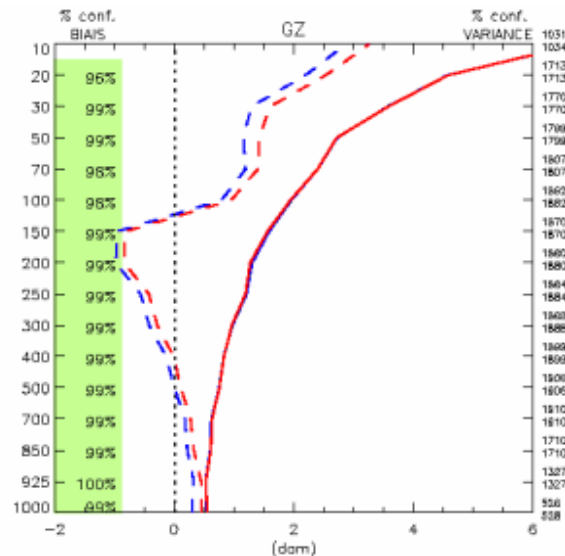


Figure 6: As Fig. 5 but for GZ and O-F, where F is a 6h forecast.

## 7.2 Impacts on regional 00h-48h forecasts

Changes in initial conditions (analyses), such as seen in section 7.1, have direct impact on forecasts through the model dynamics (advection and vertical transport of the changes). However, modifications to initial humidity fields have an added impact on forecasts through the model's moist physics (e.g. clouds and precipitation development), which in turn impacts the dynamics (winds) through associated diabatic heating and cooling. These indirect effects are highly dependent on the active weather-producing features over the experiment period and their sensitivity to changes in the evolving 3D moisture field.

Fig. 7 shows the SD of the PW differences between the control (RAM27) and experiment (RGP27) 48h forecasts. The analysis impact on PW (moisture) seen in Fig. 2 has spread eastward over the Atlantic Ocean, as well as over the Gulf of Mexico. Typical PW differences (5-10 mm) are also higher. There are still

differences over the CONUS even after 48h, and some impact is now evident over Canada.

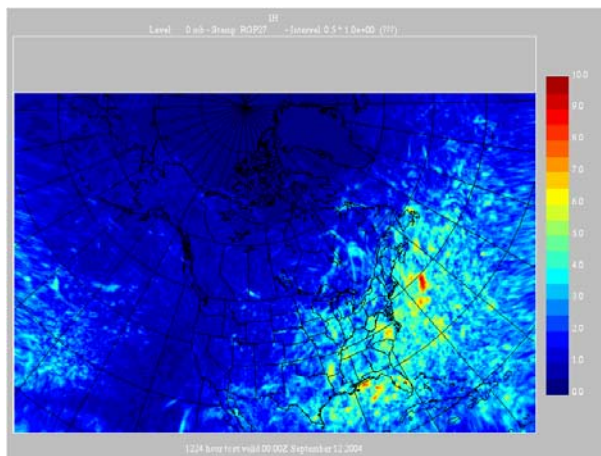


Figure 7: SD of Experiment minus Control 48h forecast PW differences (units = mm). The scale ranges between 0 and 10 mm.

The largest experiment minus control SD differences in mean layer RH after 48h are found in the middle troposphere layer (Fig. 8), and are as high as 10-20%. This is probably due to an overall upward transport of low-level humidity over the period. Convection can also produce significant changes in temperature and RH fields at mid-levels. In addition, forecast humidity errors are typically higher at mid-levels, so mid-level RH forecasts may be more sensitive to changes in initial conditions.

After 48h, the regions of mean experiment minus control differences (biases) in PW and RH (not shown) become less organized but with locally higher values compared to the analysis biases (mostly over the ocean).

Verification of the forecasts with North American radiosonde observations shows an overall neutral to slightly positive impact of GPS observations. Impact is more evident over certain regions and for certain forecast hours. For example, a positive impact is noted in lower tropospheric zonal and meridional winds, geopotential height bias, and in middle layer DPD for 36h forecasts in the southeast US (Fig. 9).

The 00-48h forecasts are verified against GPS observations of ZTD, PW,  $P_s$ ,  $T_s$  and RHs from the NOAA/ESRL network. The RHs observations are converted to surface specific humidity for comparison with that forecast. The 00h forecast is the analysis (A) used to initialize the forecast.

Verification of PW is shown in Fig. 10. Unsurprisingly, analysis PW with GPS data assimilated verifies better with the GPS observations (O), with SD O-A of 2.6 mm compared to the control SD O-A of 3.4 mm (a 24% improvement). The bias is also reduced significantly. The percent improvement in forecast PW (SD O-F) is ~8% for 12h and fairly constant at ~4% from 24-48h. The difference in forecast PW bias between the control and the experiment with GPS diminishes with time. These results are very similar to those obtained by

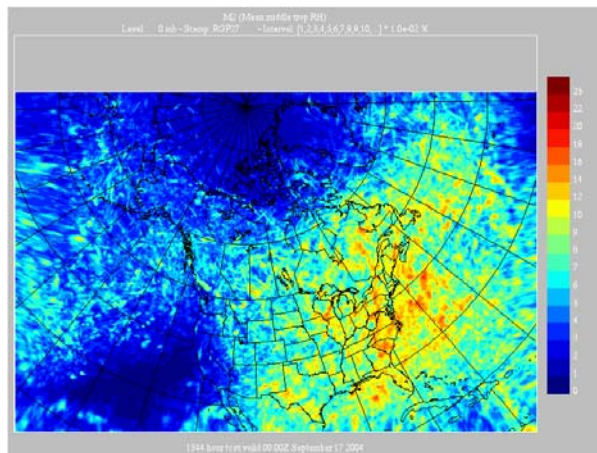


Figure 8: As Fig. 7 but for RH (units = percent). The scale ranges between 0 and 25 %.

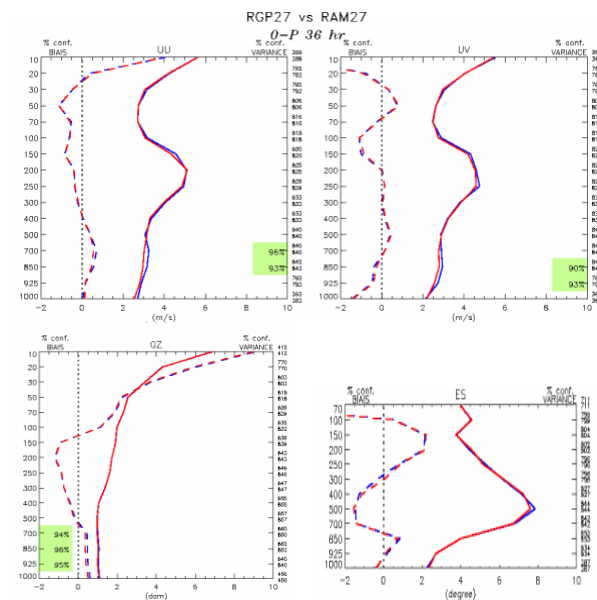


Figure 9: Verification against radiosondes of 36h forecasts over southeast US region. UU, VV are zonal and meridional winds respectively, GZ is geopotential height and ES is dewpoint depression. Red lines denote the experiment with GPS and blue lines denote the control. Dashed lines are mean (O-F) or bias and solid lines are SD (O-F).

NOAA/ESRL with GPS PW assimilation in the RUC model (section 2.2), with 25% improvement in forecast PW at 3h and 7.5% at 12h.

There is also improvement in the verification of analysis  $T_s$  and surface specific humidity when the GPS observations are assimilated (not shown), but no improvement is seen in the forecasts in this case. For  $P_s$  (Fig. 11), the analysis SD O-A for the experiment with GPS is the same as the control run, while the O-A bias is higher (by ~0.35 hPa). This bias difference is responsible for the difference in 6h forecast height (GZ) biases mentioned in section 7.1 (Fig. 6). Although the

impact on analysis  $P_s$  from GPS data assimilation is minimal, the  $P_s$  forecast (SD) error growth rate is lower in the experiment with GPS and the bias is lower as well.

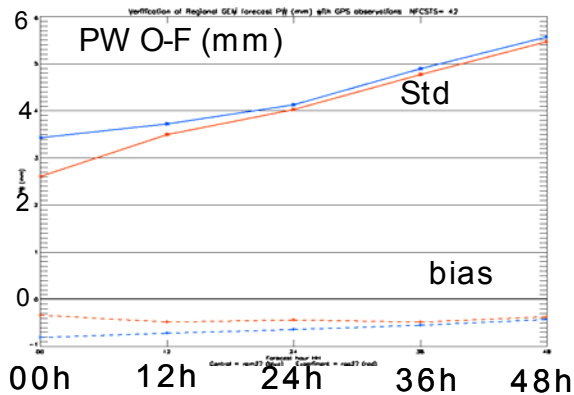


Figure 10: Verification of forecast PW (F) with observed GPS PW (O). Red lines denote the experiment with GPS and blue lines denote the control. Dashed lines are mean (O-F) or bias and solid lines are SD (O-F).

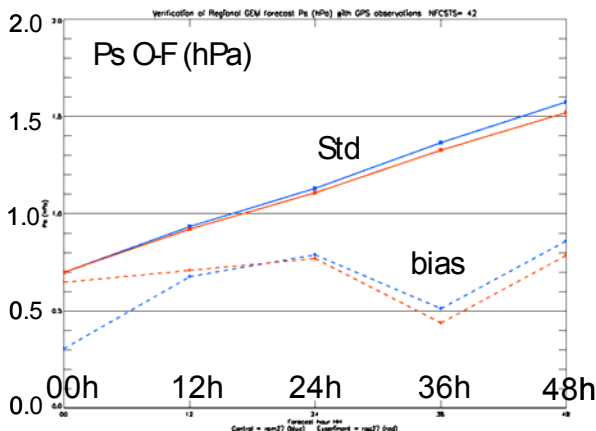


Figure 11: As Fig. 10 but for surface pressure  $P_s$ .

Verification of precipitation is done by comparing 00-24h, 12-36h and 24-48h forecast precipitation 24h accumulations with rain gauge observations. Two observation sources are used: the surface synoptic network (SYNO) and the SHEF network. The SYNO network contains sites in Canada and the US, while the SHEF network is mainly over the CONUS. There are many more stations in the SHEF network due to high site density, but most report only once a day (at 1200 UTC). Conventional categorical verification scores (Equitable Threat Score ETS, frequency bias) are computed for different amount thresholds (Joliffe and Stephenson 2003). Continuous scores (RMSE, correlation) are also computed.

The results from both SYNO and SHEF verifications show a mostly positive impact of GPS observations on GEM-REG precipitation forecasts. The

impacts tend to be greater for the higher amount thresholds and for certain regions of the US. The greatest impact is for 12-36h and 24-48h accumulations in the SHEF central US region (Fig. 12).

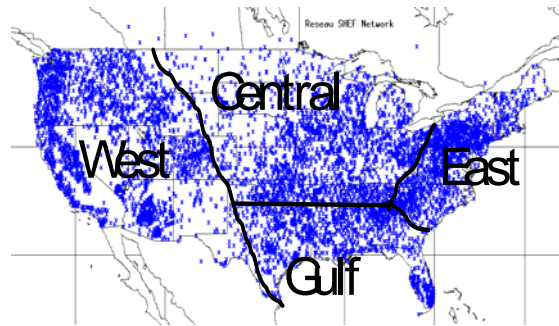


Figure 12: SHEF precipitation network.

The central region verification scores for 24-48h accumulation forecasts are shown in Figs. 13 and 14. There are improvements at all thresholds in both the ETS (Fig. 13) and frequency bias scores (Fig. 14) when GPS observations are assimilated. The correlation and RMSE scores (not shown) are also better for all three forecast lead times. The central region benefits from surrounding GPS observations on all sides except north, so there are upstream GPS observations for most prevailing flow directions.

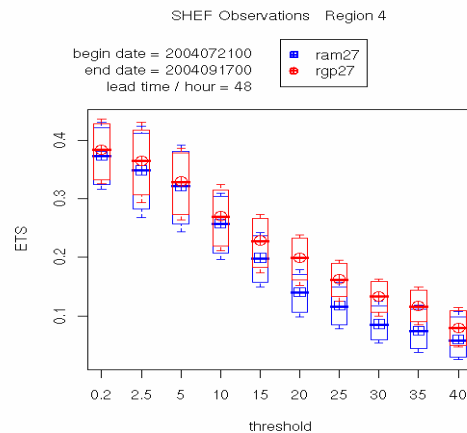


Figure 13: ETS scores for SHEF Central Region. Red (blue) represents experiment with GPS (control). Boxes show the 90% confidence intervals evaluated with a bootstrapping technique (Efron and Tibshirani 1993). Higher scores are better.

The positive impact of GPS data assimilation is most evident in particular cases rather than in the overall experiment statistics. One example is shown in Fig. 15, a 24-48h precipitation accumulation forecast ending at 1200 UTC 24 July 2004. The US radar network 24h accumulations are shown in the top part of the figure, with the experiment and control forecasts below. The GPS experiment shows a better overall accumulation pattern than the control in two regions indicated by the boxes in Fig. 15: the region of

maximum precipitation over eastern Kansas and the lack of precipitation over Indiana and Ohio.

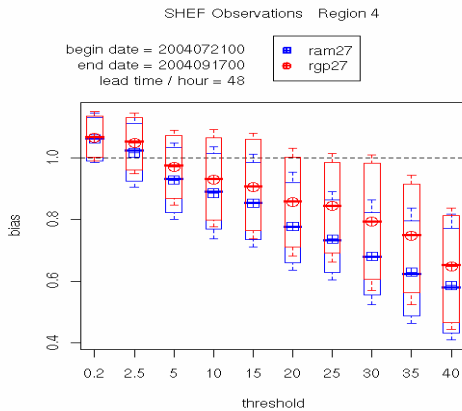


Figure 14: As Fig. 13 but for frequency bias scores. Scores greater than one diagnose over-forecasts of precipitation while scores smaller than one indicate under-forecasts.

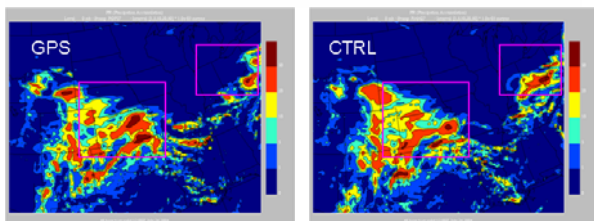
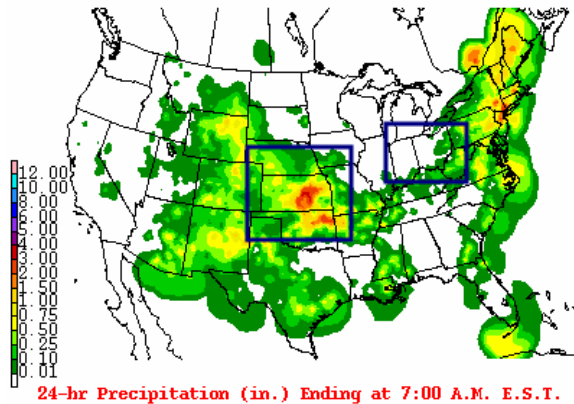


Figure 15: Top: US radar 24h precipitation accumulation ending 1200 UTC 24 July 2004, Bottom: 24-48h (24h) forecast accumulations for GPS and control experiment valid at the same time.

The experiment with GPS also gave somewhat better storm tracks than the control for the two major land-falling hurricanes that occurred during the experiment period, Frances and Ivan (both in

September 2004). The associated precipitation was also better forecast in one case (Frances). The 48h forecast hurricane tracks for Frances are shown in Fig. 16, along with the actual National Hurricane Center (NHC) track.

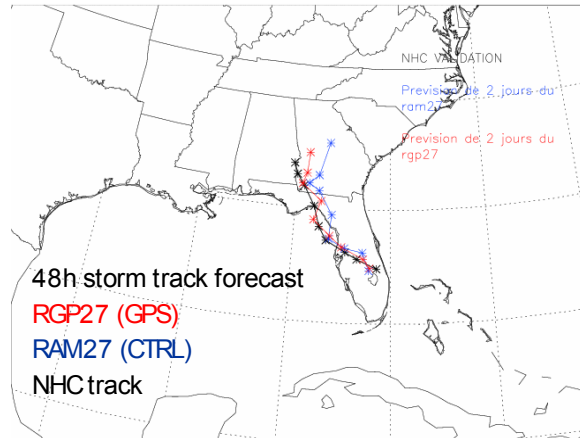


Figure 16: Two-day Hurricane Frances storm tracks: 6h positions from 1200 UTC September 5 to 1200 UTC September 7, 2004. Red (blue) represents experiment with GPS (control).

## 8. CONCLUSIONS

Ground-based GPS observations from the NOAA GPS PW network have been successfully assimilated in experiments with the EC regional analysis and forecast system. Experiments were done for summer and winter cases, but only the summer results are shown. (The impacts are smaller and more short-lived in the winter case, where mean PW over North America is much lower.) A positive impact is obtained for PW and surface pressure forecasts, as verified with GPS observations. The positive impacts extend over the entire 48h forecast period.

Systematic improvements from GPS observations on forecast 24h precipitation accumulations are also noted, especially for the 36 and 48h forecasts and for the central US region. This is due to the influence of upstream GPS observations on this region for most wind directions. Improvements in forecast precipitation accumulation are particularly evident for specific cases. This is expected, as the impact of GPS observations depends heavily on the background state and the particular weather systems that affect a region during a forecast period. There are also slight improvements in land-falling hurricane track forecasts when GPS observations are assimilated, presumably due to a better depiction of the environment encountered by the storm as it moves inland.

There is a little apparent impact on forecast upper air fields when verified (with radiosonde observations) for the US region as a whole. Although the impact is minimal, it does tend to be positive. More significant positive impacts are seen over specific regions. For example, in 36h forecast winds over the southeast US and in 48h forecast mid-tropospheric humidity over

eastern North America. In addition, impacts from GPS observations at analysis time spread over the Atlantic and Gulf regions during forecast integration, where there are no reporting stations for verification.

Ideally, the GPS observations should be assimilated in both the regional 3D-Var system and the global 4D-Var system that provides the initial analyses to the regional system. Also, the 4D-Var system would take better advantage of the high temporal frequency of the observations. Unfortunately, resource constraints did not allow this. Even so, our results with 3D-Var FGAT assimilation of GPS observations in the regional system are encouraging, and consistent with those from similar data impact studies in the US and Europe.

## 9. ACKNOWLEDGEMENTS

The authors thank Mark Buehner and Stéphane Laroche for their input on observation error correlation in time. We also thank the NOAA/ESRL/GSD for making the data from their research network available to us.

## 10. REFERENCES

- Benjamin, S.G. and Coauthors, 2004: An hourly assimilation-forecast cycle: The RUC, *Mon. Wea. Rev.*, **132**, 495–518.
- Bevis, M., S. Businger, T.A. Herring, C. Rocken, R.A. Anthes and R.H. Ware, 1992: GPS Meteorology: Remote sensing of atmospheric water vapor using the Global Positioning System, *J. Geophys. Res.*, **97** D14, 15787–15801.
- Bevis, M., S. Businger, S. Chiswell, T. Herring, R. Anthes, C. Rocken, and R. Ware, 1994: GPS Meteorology: Mapping Zenith Wet Delays onto Precipitable Water, *J. Appl. Meteor.*, **33**, 379–386.
- Bélair, S., J. Mailhot, C. Girard, and P. Vaillancourt, 2005: Boundary layer and shallow cumulus clouds in a medium-range forecast of a large-scale weather system, *Mon. Wea. Rev.*, **133**, 1938–1960.
- Côté, J., S. Gravel, A. Méthot, A. Pantoine, M. Roch, and A. Staniforth, 1998: The operational CMC/MRB global environmental multiscale (GEM) model: Part I - Design considerations and formulation. *Mon. Wea. Rev.*, **126**, 1373–1395.
- Deblonde, G., S. Macpherson, Y. Mireault and P. Héroux, 2005: Evaluation of GPS precipitable water over Canada and the IGS network, *J. Appl. Meteor.*, **44**, 153–166.
- Efron B. and R.J. Tibshirani, 1993: *An Introduction to Bootstrap*. Chapman and Hall, 436 pp.
- Eresmaa, R., and H. Järvinen, 2005: Estimation of spatial Global Positioning System zenith delay observation error covariance, *Tellus*, **57A**, 194–203.
- Foster, J., M. Bevis and S. Businger, 2005: GPS Meteorology: Sliding-window analysis, *J. Atmos. Oceanic Technol.*, **22**, 687–695.
- Gutman, S.I., S.R. Sahn, S.G. Benjamin, B.E. Schwartz, K.L. Holub, J.Q. Stewart, and T.L. Smith, 2004: Rapid retrieval and assimilation of ground based GPS precipitable water observations at the NOAA Forecast Systems Laboratory: Impact on weather forecasts. *J. Meteor. Soc. Japan*, **82**, 351–360.
- Higgins, M., 1999: Simulated 1D-variational assimilation of ground based GPS measurements of total zenith delay, *UK Met Office NWP Forecasting Research Technical Report No. 285*, 24 pp.
- Järvinen, H., E. Andersson, and F. Bouttier, 1999: Variational assimilation of time sequences of surface observations with serially correlated errors, *Tellus*, **51A**, 469–488.
- Jolliffe, I.T. and D.B. Stephenson, eds., 2003: *Forecast Verification: A Practitioner's guide in Atmospheric Science*. John Wiley and Sons, 240 pp.
- King, R.W., and Y. Bock, 2000: *Documentation for the GAMIT GPS Analysis Software Version 10.03*. Massachusetts Institute of Technology, 206 pp.
- Mailhot, J. and Coauthors, 2006: The 15-km version of the Canadian regional forecast system, *Atmos. Ocean*, **44**, 133–149.
- St.-James, J., and S. Laroche, 2005: Assimilation of wind profiler data in the Canadian Meteorological Centre's analysis systems, *J. Atmos. Oceanic Technol.*, **22**, 1181–1194.
- Stoew, B., and G. Elgered, 2005: Spatial and temporal correlations of the GPS estimation errors, *TOUGH report* (<http://web.dmi.dk/pub/tough/deliverables/d22-report.pdf>), 22 pp.
- Vedel, H. and K. Sattler, 2006: Comparison of TOUGH impact studies with ground-based GPS observations, *TOUGH report* (<http://web.dmi.dk/pub/tough/deliverables/d49-compare-results.pdf>), 18 pp.